

Supplementary Information

Supplementary Data

Analogs of erlotinib with modified aniline moieties are not sufficient to overcome T790M-mediated resistance in vitro

X-ray crystallographic studies of the EGFR-erlotinib complex have shown that erlotinib lies with the N1- and C8-containing edge of the quinazoline directed toward the peptide segment connecting the N- and C-lobes of the kinase (1) . The ether linkages (“left-hand” side) project past the connecting segment into the solvent accessible surface, while the aniline substituent on the opposite end (“right-hand” side) is sequestered in a hydrophobic pocket (**Figure 1, Supplementary Figure 1**). The ability of erlotinib to sit in this pocket is impaired when methionine is substituted for threonine at position 790. We hypothesized that analogs of erlotinib with different “right-hand” side-chains may circumvent hindrance introduced by the methionine residue. Thus, we designed and prepared a library of 22 analogs of erlotinib (all soluble in DMSO) with different right-hand side chains on the C4-quinazoline moiety (**Supplementary Figure 2**). We then determined whether 1 micromolar concentrations of any of these derivatives could inhibit the in vitro proliferation of H1975 cells, which harbor both the drug-sensitive L858R and drug-resistant T790M mutations. As a reference, we also tested the ability of these compounds to inhibit the growth of H3255 cells, which harbor only the drug-sensitive L858R missense mutation (2). We

used the irreversible inhibitors CL-387,785, EKB-569, and HKI-272, as positive controls to inhibit the growth of H1975 cells (3-5).

The majority of erlotinib analogs inhibited the growth of H3255 cells (**Supplementary Figure 3A**), suggesting they were still effective EGFR inhibitors. However, none significantly reduced the viability of H1975 cells (**Supplementary Figure 3B**). Even analogs containing thio functionalities with potential affinity for the methionine side chain (i.e. compounds EGFR-3, -12, and -13; (**supplementary Figure 2**)) did not show activity. Furthermore, when tested against H3255 cells, 5 analogs were inactive (i.e. compounds EGFR -4, -11, -13, -14, and -18). Analysis of the structures of these 5 compounds suggest that 1) there is steric tolerance within the drug-binding pocket for only small groups at the carbon 4' (para) position of the aniline aromatic ring, and 2) bulky ortho and meta substitution of the aniline ring decreases activity. Even the relatively small acetylenic group on erlotinib itself is no longer tolerated at the carbon 3' (meta) position. Taken together, results from this small library of erlotinib analogs suggest that the substituted methionine at position 790 exerts a profound stereoelectronic effect that cannot be overcome by modifying aniline moieties on erlotinib itself.

Supplementary Figure Legends

Supplementary Figure 1. Chemical structure of erlotinib.

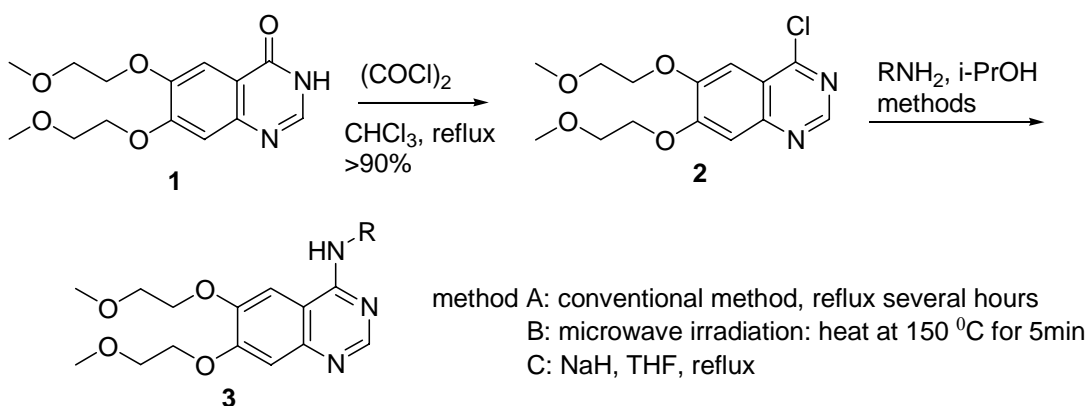
Supplementary Figure 2. Chemical structures of erlotinib analogs.

Supplementary Figure 3. Analogs of Erlotinib with Modified Aniline Moieties are Not Sufficient to Overcome T790M-Mediated Resistance in vitro. The viability of H3255 cells (A), which contain the L858R mutation alone, and H1975 cells (B), which contain both the L858R and T790M mutations, was determined after growth in various EGFR TKIs and erlotinib derivatives (supplemental Figure 1) at 1 micromolar final concentration. Only the irreversible TKIs, CL-387,785, EKB-569, and HKI-272, inhibited the growth of H1975 cells.

Supplementary Methods

Cell Culture. The NSCLC cell lines H3255 and H1975 were assayed as published (6), except that cells were seeded at a density of 1,000 cells per well in 96-well Packard ViewPlates (Perkin Elmer, Wellesley, MA) directly into inhibitors, in complete growth media (RPMI-1640 supplemented with 10% FBS and standard antibiotics). Three days after seeding, alamarBlue™ dye (Serotec, Oxford, UK) was added directly to the cells at a final concentration of 10% (vol/vol) for 4 h. AlamarBlue™ fluorescence (Ex: 531 nm, Em: 595 nm) was measured using a Victor V™ fluorescence plate reader (Perkin Elmer). Each condition was assayed in triplicate determinations, in three independent experiments.

Synthesis of Erlotinib Analogs

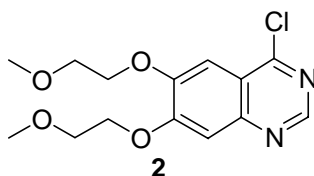


A straightforward two-step synthetic route was used to generate 6,7-Bis(2-methoxy-ethoxy)-quinazoline derivatives **3** and is depicted in Scheme 1. 6,7-Bis(2-methoxy-ethoxy)-quinazolone **1** is commercially available from Maybridge (GK03533). Chlorination of **1** with oxalyl chloride gave **2**, which was treated with the corresponding amines to provide **3** by method A, B or C.

Experimental Section

Chemistry

General. All reagents and solvents were obtained from commercial suppliers and were used without further purification. Melting points were measured with a Fisher Scientific melting point apparatus and were uncorrected. ^1H NMR and ^{13}C NMR spectra were recorded on Bruker AMX-400 MHz NMR spectrometer. Chemical shifts are given in parts per million (ppm) using tetramethylsilane as the internal standard for spectra obtained in $\text{DMSO-}d_6$ and CDCl_3 . Low-resolution mass spectral analyses were performed with a Sciex100 mass spectrometer or Waters Micromass ZQ mass spectrometer. Monitoring of reactions was carried out using Merck 60 F₂₅₄ silica gel, glass-supported TLC plates, and visualization with UV light (254 and 365 nm). Column chromatography was performed on an ISCO CombiFlash using RediSep Column.



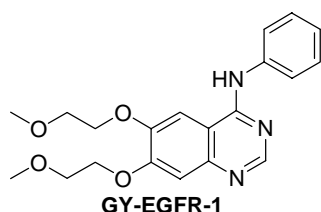
4-Chloro-6,7-bis(2-methoxy-ethoxy)-quinazoline (2). To a solution of 6,7-bis(2-methoxy-ethoxy)-quinazolone **1** (2 g, 6.8 mmol, from Maybridge) in CHCl_3 (40 mL) containing DMF (0.2 mL) was added oxalylchloride (2 mL, 22.9 mmol) dropwise over 10 min. Once foaming ceased the solution was refluxed for 2 hours. The solvent was removed in vacuo and the residue was dissolved in 1,2-dichloroethane (80 mL) and washed twice with 100 mL saturated aqueous NaHCO_3 . The organic phase was dried over Na_2SO_4 , and concentrated in vacuo to afford solid title product (2.1 g, 90%; M.P. $108^\circ\text{-}109^\circ\text{ C}$). ^1H NMR (CDCl_3) δ 8.85 (s, 1H), 7.43 (s, 1H), 7.32 (s, 1H), 4.33 (t, $J = 4.7$ Hz, 4H), 3.89 (t, $J = 4.7$ Hz, 4H), 3.50 (s, 3H), 3.49 (s, 3H); ^{13}C NMR (CDCl_3) δ 159.4, 156.7, 152.8, 151.3, 149.4, 119.9, 108.1, 104.5, 70.9, 70.7, 69.3, 69.2, 59.8; ES MS m/z 313 ($\text{M}+\text{H}$) $^+$, calculated for $\text{C}_{14}\text{H}_{17}\text{ClN}_2\text{O}_4$: 312.09.

General Procedure for method A: A mixture of **2** (160 mg, 0.48 mmol) and aniline (50 μL , 0.53 mmol) were reacted in refluxing *i*-PrOH (5 mL) under an atmosphere of Ar for 1 hr, when yellowish solid was obtained. The reaction mixture was cooled to ambient temperature, and the resulting precipitate was collected and washed with MeOH and water. The yellow solid was filtered to give **GY-EGFR-1** (160 mg, 90%).

General Procedure for method B: Microwave Irradiation Experiments. All Microwave Irradiation Experiments were carried out using [Initiator™ Microwave](#)

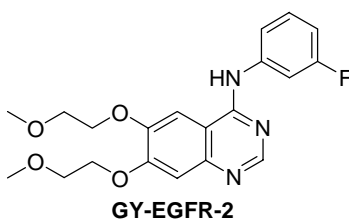
Synthesizer from Biotage. All experiments were carried out in sealed microwave process vials utilizing the standard absorbance level (300 W maximum power). A mixture of 0.1 mmol (31 mg) of **2**, 0.11 mmol (14 μ L, 1.1 equiv) of 3-methylthioaniline and 1.0 mL of *i*-PrOH was irradiated under microwave conditions at 150 °C for 5 min in a 2-5 mL microwave process vial. To the formed yellow precipitate, 200 μ L of H₂O was added and the formed precipitate was separated by filtration, washed with *i*-PrOH and finally twice with 0.5 mL of Et₂O, to give 29 mg of product as a yellow solid (78% yield).

General Procedure for method C. To a solution of **2** (500 mg, 0.16 mmol) and 2,6-dibromo-3-chloro-4-fluorobenzenamine (100 mg, 0.32 mmol) in THF (5 mL), NaH (15 mg, 60% in mineral oil) was added. The mixture was refluxed for 18 hr. The mixture was cooled to room temperature and partitioned between water and EtOAc. The organic layer was dried over MgSO₄, filtered and concentrated in vacuo. The residue was purified by flash chromatography eluting with MeOH/CH₂Cl₂ (5 -10%) to provide 19 mg (20 %) of product.

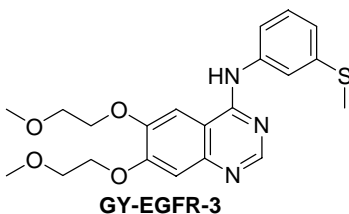


6,7-Bis(2-methoxyethoxy)-N-phenylquinazolin-4-amine Hydrochloride (GY-EGFR-1). Yellow solid (90% yield, method A): M.P. 238°-240° C ; ¹H NMR (DMSO-*d*₆) δ 11.30 (br s, 1H), 8.78 (s, 1H), 8.31 (s, 1H), 7.66 (d, *J* = 7.5 Hz, 2H),

7.47 (t, $J = 7.6$ Hz, 2H), 7.35 (s, 1H), 7.31 (t, $J = 7.3$ Hz, 1H), 4.34 (m, 4H), 3.76 (m, 4H), 3.37 (s, 3H), 3.34 (s, 3H); ES MS m/z 370 ($M + H$)⁺, calculated for $C_{20}H_{23}N_3O_4$: 369.17.

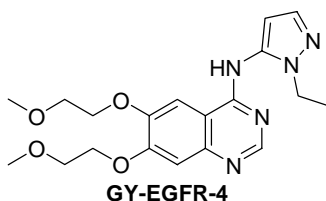


6,7-Bis(2-methoxyethoxy)-N-(3-fluorophenyl)quinazolin-4-amine (GY-EGFR-2). White solid (81% yield, method A); M.P. 235^o-238^o C ; ¹H NMR (DMSO-*d*₆) δ 11.23 (br s, 1H), 8.87 (s, 1H), 8.29 (s, 1H), 7.72 (d, $J = 11.1$ Hz, 1H), 7.54 (m, 2H), 7.36 (s, 1H), 7.16 (t, $J = 8.2$ Hz, 1H), 4.36 (m, 4H), 3.80 (m, 4H), 3.38 (s, 3H), 3.37 (s, 1H); ES MS m/z 388 ($M + H$)⁺, calculated for $C_{20}H_{22}FN_3O_4$: 387.16.



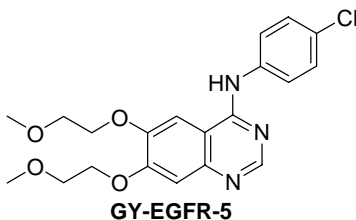
6,7-Bis(2-methoxyethoxy)-N-(3-(methylthio)phenyl)quinazolin-4-amine Hydrochloride (GY-EGFR-3). Yellow solid (78% yield, method B). M.P. 222^o-223^o C ; ¹H NMR (DMSO-*d*₆) δ 11.06 (br s, 1H), 8.83 (s, 1H), 8.21 (s, 1H), 7.61 (s, 1H), 7.46 (m, 2H), 7.32 (s, 1H), 7.21 (d, $J = 7.0$ Hz, 1H), 4.36 (m, 4H), 3.80

(m, 4H), 3.38 (s, 3H), 3.37 (s, 3H), 2.68 (s, 3H); ES MS m/z 416 (M + H)⁺, calculated for C₂₁H₂₅N₃O₄S: 415.16.



6,7-Bis(2-methoxyethoxy)-N-(1-ethyl-1H-pyrazol-5-yl)quinazolin-4-amine

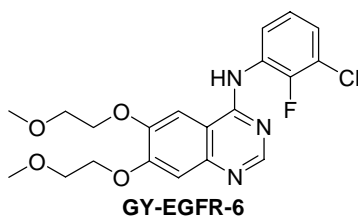
(GY-EGFR-4). Yellow solid (30 % yield, method B, heat at 180 °C for 5 min, two drop of 1 N HCl in ether was added). ¹H NMR (CDCl₃) δ 8.51 (br, 1H), 7.55 (s, 1H), 7.35 (br, 1H), 7.19 (s, 1H), 6.19 (br, 1H), 4.21 (m, 4H), 4.07 (q, $J = 6.9$ Hz, 2H), 3.81 (m, 4H), 3.45 (s, 3H), 3.43 (s, 3H), 1.41 (t, $J = 7.2$ Hz, 3H); ES MS m/z 388 (M + H)⁺, calculated for C₁₉H₂₅N₅O₄: 387.19.



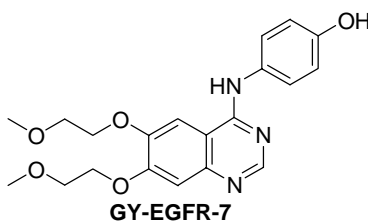
6,7-Bis(2-methoxyethoxy)-N-(4-chlorophenyl)quinazolin-4-amine

hydrochloride (GY-EGFR-5). Yellow solid (88 % yield, method B, heat at 170 °C for 5 min). M.P. 260°-262° C; ¹H NMR (DMSO-*d*₆) δ 11.14 (br, s, 1H), 8.82 (s, 1H), 8.23 (s, 1H), 7.75 (d, $J = 8.7$ Hz, 2H), 7.56 (d, $J = 8.7$ Hz, 2H), 7.33 (s, 1H),

4.35 (m, 4H), 3.79 (m, 4H), 3.36 (s, 3H), 3.35 (s, 3H); ES MS m/z 404 (M + H)⁺, calculated for C₂₀H₂₂ClN₃O₄: 403.13.

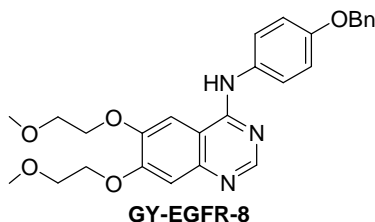


6,7-Bis(2-methoxyethoxy)-N-(3-chloro-2-fluorophenyl)quinazolin-4-amine hydrochloride (GY-EGFR-6). Yellow solid (50 % yield, method B, heat at 170 °C for 5 min). M.P. 225°-228° C ; ¹H NMR (DMSO-*d*₆) δ 11.35 (br, s, 1H), 8.92 (s, 1H), 8.28 (s, 1H), 7.77 (t, *J* = 7.5 Hz, 1H), 7.69 (t, *J* = 7.3 Hz, 1H), 7.50 (t, *J* = 8.1 Hz, 1H), 7.45 (s, 1H), 4.47 (m, 4H), 3.91 (m, 4H), 3.50 (s, 3H), 3.49 (s, 3H); ES MS m/z 422 (M + H)⁺, calculated for C₂₀H₂₁ClFN₃O₄: 421.12.



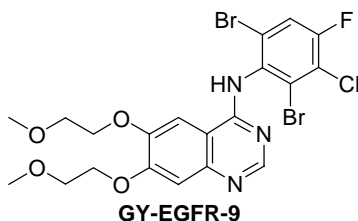
4-(6,7-Bis(2-methoxyethoxy)quinazolin-4-ylamino)phenol (GY-EGFR-7). Yellow solid (90 % yield, method B, heat at 160 °C for 5 min). M.P. 236°-238° C ; ¹H NMR (DMSO-*d*₆) δ 11.14 (br s, 1H), 9.67 (s, 1H), 8.73 (s, 1H), 8.19 (s, 1H), 7.42 (d, *J* = 8.6 Hz, 2H), 7.31 (s, 1H), 6.87 (d, *J* = 8.6 Hz, 2H), 4.32 (m, 4H), 3.78

(m, 4H), 3.36 (s, 6H), ES MS m/z 386 ($M + H$)⁺, calculated for C₂₀H₂₃N₃O₅: 385.16.



6,7-Bis(2-methoxyethoxy)-N-(4-(benzyloxy)phenyl)quinazolin-4-amine

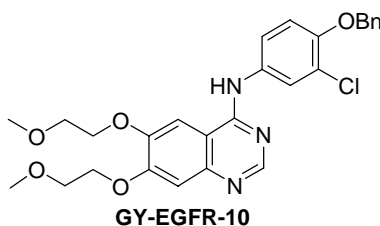
hydrochloride (GY-EGFR-8). Yellow solid (70%, method B, heat at 160 °C for 5 min). M.P. 216°-220° C ; ¹H NMR (DMSO-*d*₆) δ 11.13 (br, s, 1H), 8.75 (s, 1H), 8.21 (s, 1H), 7.56 (d, *J* = 8.8 Hz, 2H), 7.48 (d, *J* = 7.9 Hz, 2H), 7.41 (t, *J* = 7.8 Hz, 2H), 7.36 (d, *J* = 6.6 Hz, 1H), 7.31 (s, 1H), 7.13 (d, *J* = 8.4 Hz, 2H), 5.16 (s, 2H), 4.33 (m, 4H), 3.78 (m, 4H), 3.36 (s, 3H), 3.35 (s, 3H); ES MS m/z 476 ($M + H$)⁺, calculated for C₂₇H₂₉N₃O₅: 475.21.



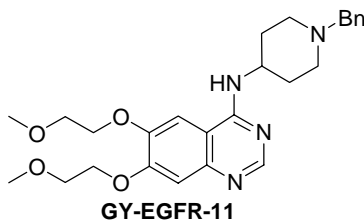
6,7-Bis(2-methoxyethoxy)-N-(2,6-dibromo-3-chloro-4-

fluorophenyl)quinazolin-4-amine (GY-EGFR-9). 20% yield, method C. ¹H NMR (CDCl₃) δ 8.54 (s, 1H), 7.72 (br s, 1H), 7.54 (d, *J* = 7.8 Hz, 1H), 7.35 (s, 1H), 7.26

(d, $J = 7.6$ Hz, 1H), 4.26 (m, 2H), 4.14 (m, 2H), 3.83 (m, 2H), 3.76 (m, 2H), 3.46 (s, 3H), 3.43 (s, 3H); ES MS m/z 578 ($M + H$)⁺, calculated for C₂₀H₁₉Br₂ClFN₃O₄: 576.94.

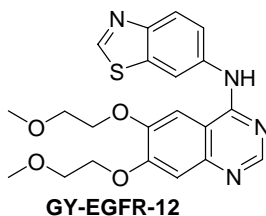


6,7-Bis(2-methoxyethoxy)-N-(4-(benzyloxy)-3-chlorophenyl)quinazolin-4-amine hydrochloride (GY-EGFR-10). Yellow solid (70%, method B, heat at 160 °C for 5 min). M.P. 223°-226° C ; ¹H NMR (DMSO-*d*₆) δ 11.03 (br, s, 1H), 8.82 (s, 1H), 8.17 (s, 1H), 7.85 (d, $J = 2.3$ Hz, 1H), 7.61 (dd, $J = 2.1, 8.8$ Hz, 1H), 7.52 (s, 1H), 7.50 (s, 1H), 7.44 (t, $J = 7.6$ Hz, 2H), 7.37 (m, 2H), 7.31 (s, 1H), 5.29 (s, 2H), 4.35 (m, 4H), 3.79 (m, 4H), 3.38 (s, 3H), 3.37 (s, 3H); ES MS m/z 510 ($M + H$)⁺, calculated for C₂₇H₂₈ClN₃O₅: 509.17.



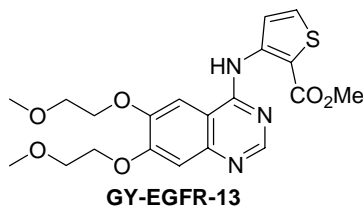
6,7-Bis(2-methoxyethoxy)-N-(1-benzylpiperidin-4-yl)quinazolin-4-amine (GY-EGFR-11). White solid (40%, method B, heat at 160 °C for 5 min). ¹H NMR

(CDCl₃) δ 8.53 (s, 1H), 7.33-7.25 (m, 5H), 7.15 (s, 1H), 7.08 (s, 1H), 5.52 (d, J = 7.6 Hz, 1H), 4.24 (m, 5H), 3.79 (m, 4H), 3.61 (s, 2H), 3.45 (s, 3H), 3.44 (s, 3H), 2.93 (d, J = 11.5 Hz, 2H), 2.25 (t, J = 11.2 Hz, 2H), 2.13 (d, J = 10.5 Hz, 2H), 1.67 (m, 2H); ES MS m/z 467 (M + H)⁺, calculated for C₂₆H₃₄N₄O₄: 466.26.



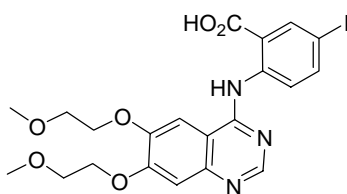
6,7-Bis(2-methoxyethoxy)-N-(benzo[d]thiazol-6-yl)quinazolin-4-amine

hydrochloride (GY-EGFR-12). Yellow solid (73%, method B, heat at 160 °C for 5 min). M.P. 125°-126° C; ¹H NMR (DMSO-*d*₆) δ 9.68 (s, 1H), 9.31 (s, 1H), 8.72 (d, J = 1.9 Hz, 1H), 8.51 (s, 1H), 8.11 (d, J = 8.8 Hz, 1H), 7.93 (s, 1H), 7.87 (dd, J = 2.0, 8.8 Hz, 1H), 7.25 (s, 1H), 4.31 (m, 4H), 3.77 (m, 4H), 3.38 (s, 3H), 3.36 (s, 3H); ES MS m/z 427 (M + H)⁺, calculated for C₂₁H₂₂N₄O₄S: 426.14.



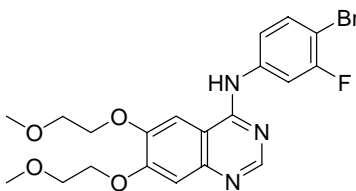
Methyl 3-(6,7-bis(2-methoxyethoxy)quinazolin-4-ylamino)thiophene-2-carboxylate (GY-EGFR-13). Yellow solid (36%, method B, heat in *t*-BuOH at

180 °C for 7 min). M.P. 155°-157° C ; $^1\text{H NMR}$ (CDCl_3) δ 10.88 (s, 1H), 9.15 (s, 1H), 8.60 (d, $J = 5.5$ Hz, 1H), 7.52 (d, $J = 5.5$ Hz, 1H), 7.32 (s, 1H), 7.24 (s, 1H), 4.38 (t, $J = 4.5$ Hz, 2H), 4.30 (t, $J = 4.5$ Hz, 2H), 3.95 (s, 3H), 3.92 (t, $J = 4.9$ Hz, 2H), 3.87 (t, $J = 5.0$ Hz, 2H), 3.52 (s, 3H), 3.49 (s, 3H); ES MS m/z 434 ($\text{M} + \text{H}$) $^+$, calculated for $\text{C}_{20}\text{H}_{23}\text{N}_3\text{O}_6\text{S}$: 433.13.



GY-EGFR-14

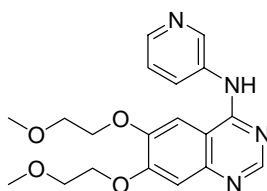
2-(6,7-Bis(2-methoxyethoxy)quinazolin-4-ylamino)-5-iodobenzoic acid (GY-EGFR-14). Yellow solid (40%, method B, heat at 150 °C for 5 min). M.P. 245°-248° C ; $^1\text{H NMR}$ ($\text{DMSO-}d_6$) δ 9.28 (s, 1H), 8.58 (s, 1H), 8.23 (d, $J = 8.8$ Hz, 1H), 8.13 (s, 1H), 7.64 (d, $J = 8.5$ Hz, 1H), 7.44 (s, 1H), 4.38 (m, 4H), 3.78 (m, 4H), 3.38 (s, 3H), 3.36 (s, 3H); ES MS m/z 540 ($\text{M} + \text{H}$) $^+$, calculated for $\text{C}_{21}\text{H}_{22}\text{IN}_3\text{O}_6$: 539.06.



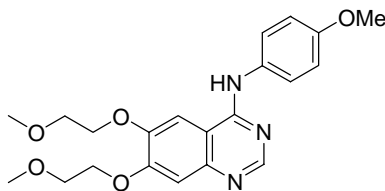
GY-EGFR-15

6,7-Bis(2-methoxyethoxy)-N-(4-bromo-3-fluorophenyl)quinazolin-4-amine

hydrochloride (GY-EGFR-15). Yellow solid (67%, method B, heat at 160 °C for 5 min). M.P. 245°-248° C ; ¹H NMR (DMSO-*d*₆) δ 11.15 (br s, 1H), 8.88 (s, 1H), 8.25 (s, 1H), 7.97 (dd, *J* = 2.1, 10.8 Hz, 1H), 7.83 (t, *J* = 8.4 Hz, 1H), 7.61 (d, *J* = 8.3 Hz, 1H), 7.34 (s, 1H), 4.37 (m, 4H), 3.80 (m, 4H), 3.38 (s, 3H), 3.37 (s, 3H); ES MS *m/z* 466 (M + H)⁺, calculated for C₂₀H₂₁BrFN₃O₄: 465.07.

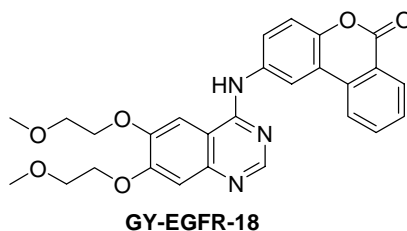
**GY-EGFR-16****6,7-Bis(2-methoxyethoxy)-N-(pyridin-3-yl)quinazolin-4-amine (GY-EGFR-16).**

Yellow solid (38%, method B, heat at 160 °C for 5 min). ¹H NMR (CDCl₃) δ 8.78 (br s, 1H), 8.64 (s, 1H), 8.40 (m, 2H), 7.86 (s, 1H), 7.36 (m, 1H), 7.34 (s, 1H), 7.21 (s, 1H), 4.23 (t, *J* = 4.5 Hz, 2H), 4.19 (t, *J* = 4.5 Hz, 2H), 3.82 (t, *J* = 4.8 Hz, 2H), 3.77 (t, *J* = 4.6 Hz, 2H), 3.43 (s, 3H), 3.42 (s, 3H); ES MS *m/z* 371 (M + H)⁺, calculated for C₁₉H₂₂N₄O₄: 370.16.

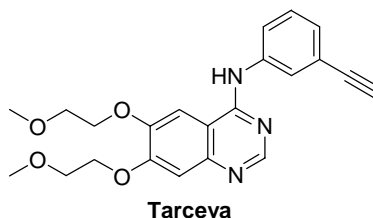
**GY-EGFR-17**

6,7-Bis(2-methoxyethoxy)-N-(4-methoxyphenyl)quinazolin-4-amine**hydrochloride**

(GY-EGFR-17). Yellow solid (37%, method B, heat at 160 °C for 5 min). M.P. 180°-181° C; ¹H NMR (CDCl₃) δ 8.55 (br s, 1H), 8.04 (br s, 1H), 7.50 (d, *J* = 8.8 Hz, 2H), 7.35 (m, 1H), 7.14 (s, 1H), 6.88 (d, *J* = 8.8 Hz, 2H), 4.15 (m, 4H), 3.76 (s+m, 5H), 3.66 (m, 2H), 3.39 (s, 3H), 3.36 (s, 3H); ES MS *m/z* 400 (M + H)⁺, calculated for C₂₁H₂₅N₃O₆: 399.18.

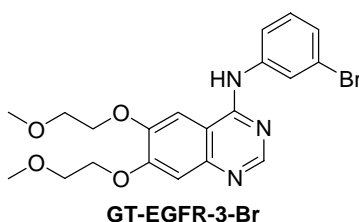
**2-(6,7-Bis(2-methoxyethoxy)quinazolin-4-ylamino)-6H-benzo[c]chromen-6-one**

(GY-EGFR-18). Gray solid (37%, method B, heat in t-BuOH at 180 °C for 7 min). M.P. 260°-263° C; ¹H NMR (DMSO-d₆) δ 11.53 (br s, 1H), 8.92 (s, 1H), 8.74 (s, 1H), 8.47 (d, *J* = 8.0 Hz, 1H), 8.40 (m, 1H), 8.37 (s, 1H), 8.07 (d, *J* = 7.5 Hz, 1H), 7.95 (d, *J* = 8.7 Hz, 1H), 7.82 (t, *J* = 7.5 Hz, 1H), 7.65 (d, *J* = 8.6 Hz, 1H), 7.43 (s, 1H), 4.44 (m, 4H), 3.88 (m, 4H), 3.46 (s, 6H); ES MS *m/z* 488 (M + H)⁺, calculated for C₂₇H₂₅N₃O₆: 487.17.

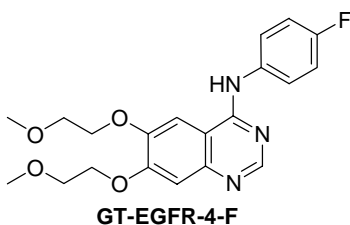


6,7-Bis(2-methoxyethoxy)-N-(3-ethynylphenyl)quinazolin-4-amine

Hydrochloride (Erlotinib). Yellow solid (87%, method B, heat at 160 °C for 5 min). M.P. 208°-210° C; ¹H NMR (DMSO-*d*₆) δ 11.04 (br s, 1H), 8.63 (s, 1H), 8.12 (s, 1H), 7.68 (s, 1H), 7.58 (d, *J* = 8.3 Hz, 1H), 7.30 (t, *J* = 7.8 Hz, 1H), 7.20 (d, *J* = 7.7 Hz, 1H), 7.16 (s, 1H), 4.16 (m, 4H), 3.59 (m, 4H), 3.17 (s, 6H); ES MS *m/z* 394 (M + H)⁺, calculated for C₂₂H₂₃N₃O₄: 393.17.

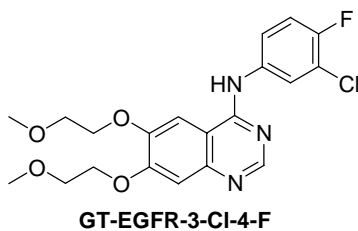
**6,7-Bis(2-methoxyethoxy)-N-(3-bromophenyl)quinazolin-4-amine**

Hydrochloride (GT-EGFR-3-Br). White solid (80%, method B, heat at 150 °C for 10 min). M.P. 228°-230° C; ¹H NMR (DMSO-*d*₆) δ 11.31 (br s, 1H), 8.87 (s, 1H), 8.32 (s, 1H), 8.02 (s, 1H), 7.78 (d, *J* = 7.8 Hz, 1H), 7.50 (m, 2H), 7.36 (s, 1H), 4.36 (m, 4H), 3.79 (m, 4H), 3.36 (s, 6H); ES MS *m/z* 448 (M + H)⁺, calculated for C₂₀H₂₂BrN₃O₄: 447.08.

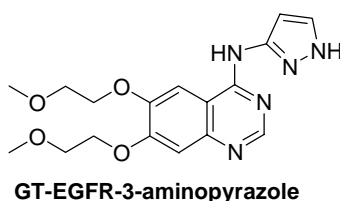


6,7-Bis(2-methoxyethoxy)-N-(4-fluorophenyl)quinazolin-4-amine

Hydrochloride (GT-EGFR-4-F). White solid (69%, method B, heat at 150 °C for 10 min). M.P. 253°-256° C; ¹H NMR (DMSO-*d*₆) δ 11.14 (br s, 1H), 8.79 (s, 1H), 8.21 (s, 1H), 7.69 (m, 2H), 7.34 (m, 3H), 4.34 (m, 4H), 3.79 (m, 4H), 3.36 (s, 6H); ES MS *m/z* 388 (M + H)⁺, calculated for C₂₀H₂₂FN₃O₄: 387.16.

**6,7-Bis(2-methoxyethoxy)-N-(3-chloro-4-fluorophenyl)quinazolin-4-amine**

Hydrochloride (GT-EGFR-3-Cl-4-F). White solid (67%, method B, heat at 150 °C for 10 min). M.P. 235°-238° C; ¹H NMR (DMSO-*d*₆) δ 11.31 (br s, 1H), 8.85 (s, 1H), 8.29 (s, 1H), 8.02 (dd, *J* = 2.5, 6.7 Hz, 1H), 7.74 (m, 1H), 7.55 (t, *J* = 9.1 Hz, 1H), 7.34 (s, 1H), 4.35 (m, 4H), 3.79 (m, 4H), 3.36 (s, 6H); ES MS *m/z* 422 (M + H)⁺, calculated for C₂₀H₂₁ClFN₃O₄: 421.12.



6,7-Bis(2-methoxyethoxy)-N-(1H-pyrazol-3-yl)quinazolin-4-amine (GT-EGFR-3-aminopyrazole). (Yellow solid 37%, method B, heat at 150 °C for 10 min). M.P. 243°-245° C; ¹H NMR (DMSO-*d*₆) δ 12.86 (br s, 1H), 11.67 (br s, 1H), 8.87 (s, 1H), 8.26 (s, 1H), 7.82 (d, *J* = 1.9 Hz, 1H), 7.30 (s, 1H), 6.84 (s, 1H), 4.32 (m, 4H), 3.78 (m, 4H), 3.36 (s, 6H); ES MS *m/z* 360 (M + H)⁺, calculated for C₁₇H₂₁N₅O₄: 359.16.

Literature Cited

1. Stamos, J., Sliwkowski, M.X., and Eigenbrot, C. 2002. Structure of the epidermal growth factor receptor kinase domain alone and in complex with a 4-anilinoquinazoline inhibitor. *J Biol Chem* 277:46265-46272.
2. Tracy, S., Mukohara, T., Hansen, M., Meyerson, M., Johnson, B.E., and Janne, P.A. 2004. Gefitinib induces apoptosis in the EGFR^{L858R} non-small cell lung cancer cell line H3255. *Cancer Res* 64:7241-7244.
3. Carter, T.A., Wodicka, L.M., Shah, N.P., Velasco, A.M., Fabian, M.A., Treiber, D.K., Milanov, Z.V., Atteridge, C.E., Biggs, W.H., Edeen, P.T., et al. 2005. Inhibition of drug-resistant mutants of ABL, KIT and EGF receptor kinases. *Proc Natl Acad Sci (USA)* 102:11011-11016.
4. Kobayashi, S., Boggon, T.J., Dayaram, T., Janne, P.A., Kocher, O., Meyerson, M., Johnson, B.E., Eck, M.J., Tenen, D.G., and Halmos, B. 2005. EGFR mutation and resistance of non-small-cell lung cancer to gefitinib. *New Engl J Med* 352:786-792.
5. Kwak, E.L., Sordella, R., Bell, D.W., Godin-Heymann, N., Okimoto, R.A., Brannigan, B.W., Harris, P.L., Driscoll, D.R., Fidias, P., Lynch, T.J., et al. 2005. Irreversible inhibitors of the EGF receptor may circumvent acquired resistance to gefitinib. *Proc Natl Acad Sci U S A* 102:7665-7670.
6. Pao, W., Miller, V.A., Politi, K.A., Riely, G.J., Somwar, R., Zakowski, M.F., Kris, M.G., and Varmus, H. 2005. Acquired resistance of lung

adenocarcinomas to gefitinib or erlotinib is associated with a second mutation in the EGFR kinase domain. *PLoS Medicine* 2:e73.